Supporting Information

Thuenauer et al. 10.1073/pnas.1304168111

SI Materials and Methods

Reagents. The following primary antibodies were used: rabbit anticalnexin (Sigma Aldrich), rabbit anti-Rab11a (Invitrogen), mouse antigiantin (LifeSpan Biosciences), rabbit anti-GFP (Abcam), mouse anti–beta-actin (Sigma Aldrich), mouse anti-dyn2 (BD Biosciences), rabbit anti–beta-catenin (Abcam), and rat anti-ZO-1 (Millipore). Secondary anti-mouse and anti-rabbit antibodies conjugated to Alexa405, Alexa488, Alexa555, and Alexa647 and anti-rat antibody conjugated to Alexa488 were purchased from Invitrogen. Secondary anti-mouse and anti-rabbit IRDye680- and IRDye800-conjugated antibodies were purchased from LI-COR. Five nanometers of colloidal gold-conjugated anti-rabbit antibodies was purchased from GE Healthcare. Mouse anti-HA antibody (Covance) was directly conjugated to Cy5 using a Cy5 conjugation kit (GE Healthcare). Adenovirus encoding dyn2-WT and dyn2-K44A (1) were purchased from University of Iowa Gene Transfer Vector Core.

Plasmids. The plasmid encoding FM4-rhodopsin-GFP was made in a multistep process. First, the human growth hormone signal sequence followed by four FM domains and a furin cleavage site were PCR amplified from the plasmid pC4S1-FM4-FCS-hGH (ARIAD) with the primer pair 5′-GACTGCTAGCGCCACCATGGCTACAGGCTCCCGGAC-3′ and 5′-CGTAAGATCTGATCTCTTCTGACGGTTTCTAGC-3′, which introduced a BmtI restriction site at the 5′ end and a BglII restriction site at the 3′ end and then cloned into pEGFP-N1 (Clontech) resulting in the intermediate plasmid pFM4-GFP. Next, GFP-tagged rhodopsin followed by a repeat of the last eight residues of rhodopsin's C terminus was PCR amplified from a previously described plasmid (2) using the primer pair 5′-GACTAAGCTTATGAATGGCACAGAAGGCCC-3′ and 5′-CGTAGCGGCCGCCTTAGGCCGGGGCCACCTG-3′, which introduced a HindIII restriction site at the 5′ end and a NotI restriction site at the 3′ end. The PCR product was then cloned into FM4-GFP resulting in the plasmid encoding FM4-rhodopsin-GFP.

Plasmids encoding GFP-tagged wild type and dominant negative Rab11a and dyn-2 were gifts from Tim McGraw (Weill Medical College of Cornell University, New York) and Pietro De Camilli (Yale University School of Medicine, New Haven, CT), respectively. The plasmid encoding Rab11b was a gift from Michael Butterworth (University of Pittsburgh, Pittsburgh) (3). The plasmids encoding Rab11a-mCherry, Rab11b-mCherry, DN-Rab11a-mCherry, dyn2-RFP, and dyn2-K44A-mCherry were generated by swapping GFP for mCherry or RFP using restriction enzyme cloning strategies. All plasmids were verified by sequencing.

Cell Culture and Stable Cell Lines. Madin-Darby canine kidney (MDCK) II cells were cultured in DMEM supplemented with 5% (vol/vol) FCS at 37 °C and 5% (vol/vol) CO_2. MDCK II cells stably expressing Rab11a-mCherry were established by transfecting WT MDCK II cells with Rab11a-mCherry by electroporation (Amaxa) followed by grams per milliliters of G418. The MDCK II cell line stably expressing ST-RFP has been previously described (4).

Lentivirus Production. Dyn2 knockdown was performed via lentivirus-mediated shRNA expression. The plasmid pLVTH (5) was modified by Gibson assembly (6) to encode for dyn2-shRNA based on the target sequence GACATGATCCTGCAGTTCA (7). The resulting plasmid, pLVTH-i-dyn2, encodes for both dyn2-shRNA and GFP. Lentiviral particles were produced by transfecting HEK 293T cells with pCMV-ΔR8.91, pMD2G-VSVG (5), and pLVTH-i-dyn2. The supernatant was collected after 3 d and lentiviral particles were concentrated with centrifugal filter units (Amicon Ultra-15 50K; Millipore) and resuspended in cell culture medium.

Immunoblotting. Subconfluent MDCK cells transfected with FM4-rhodopsin-GFP were treated with AP21998 for the indicated times and then lysed in 50 mM Tris·HCl, pH 7.4, 150 mM NaCl, 25 mM KCl, 2 mM EDTA, 1% sodium deoxycholate, 0.1% SDS, 1% Triton X-100, supplemented with 1 mM PMSF and 15 $\mu g \cdot mL^{-1}$ leupeptin/pepstatin/antipain and 37 $\mu g \cdot mL^{-1}$ benzamidine-HCl for 30 min at 4 °C. Lysates were cleared by centrifugation (18,000 × *g* for 10 min) and 20 μg of protein was subjected to standard SDS/PAGE and immunoblotting analysis. Protein bands were detected by Odyssey scanner (LI-COR).

Immunocytochemistry. For immunostaining, cells were fixed with 1% paraformaldehyde for 15 min at room temperature, followed by permeabilization in 0.1% Triton X-100 for 5 min. After blocking in 1% BSA and 0.5% Tween-20, cells were incubated with indicated primary antibodies and then with appropriate secondary antibodies conjugated to fluorescent dyes. Nuclei were counterstained with DAPI and cells were mounted in DABCO/glycerol solution.

Live Cell Confocal Imaging and Image Analysis. For experiments with polarized cells, cells were cultured on Transwell filters (polycarbonate, 0.4 μm pore size; Corning) for 4 d. On the day of measurement, cells were transfected with indicated plasmids from the apical side using Lipofectamine 2000 (Invitrogen) for 6 h and then treated with 100 μg/mL cycloheximide (Sigma) for 1 h. For measurement, the filter was cut out with a scalpel and carefully placed with the cells pointing downward on a glass coverslip. A cloning cylinder was placed on top of the filter to stabilize the cell layer in a position within the working distance of the microscope objective. For experiments with subconfluent cells, cells were sparsely seeded on eight-well chambered coverslips (Nunc Lab-Tek) and allowed to attach overnight. On the day of measurement, cells were transfected with indicated plasmids using Lipofectamine 2000 (Invitrogen) for 6 h and then treated with 100 μg/mL cycloheximide for 1 h. Imaging was done in recording medium [HBSS supplemented with 1% FBS, 4.5 g/L glucose, 100 μg/mL cycloheximide, and 5 μM AP21998 (ARIAD)] on a Axio Observer Z1 (Zeiss) equipped with a spinning disk confocal unit (CSU-X1; Yokogawa), an Orca-R2 CCD camera (Hamamatsu), a sample holder heated to 37 °C, and a 40× N.A. 1.4 objective with additional 1.6× Optovar magnification. The colocalization of FM4-rhodopsin-GFP with compartment markers was calculated as a Manders M1 coefficient (8) by using a custom-written Matlab program (MathWorks, release 12).

Cell Surface Arrival Assay. Polarized cells grown on Transwell filters were transfected from the apical side for 6 h and then treated with 100 μg/mL cycloheximide for 1 h. AP21998 was applied for 3 h and then cells were incubated with Cy5-conjugated anti-HA antibody from the apical or basolateral side for 1 h. After washes, cells were fixed and mounted. In the case of dynasore treatment, the cells were washed three times with medium without FCS before release and the further experiment was carried out with FCS-free medium. To quantify HA-rhodopsin surface arrival, confocal image stacks of the samples were taken,

and the HA-rhodopsin-GFP and anti-HA-Cy5 signals were determined for single cells by a custom-written Matlab program.

Apical Total Internal Reflection Fluorescence Microscopy and Imaging of Apical Vesicle Fusion Events. The biochip for apical total internal reflection fluorescence microscopy (TIRFM) and the cell culture procedure on the biochip have been described previously (9). Briefly, MDCK II cells were grown on the fibronectin-coated cell culture area of the polydimethylsiloxane-based biochip (9) for 4 d before transfection with indicated plasmids. Immediately before measurement, the medium was changed to recording medium. Then, the chip was transferred to the microscope and placed upside down on a BSA-coated glass slide. Imaging was done with a homemade TIRFM setup, as described previously (10). Briefly, the setup is based on an Axiovert 200 microscope (Zeiss) and equipped with a 100× N.A. 1.46 alpha-plan-apochromat objective and CoolSnap CCD cameras (Photometrics). Images were acquired with Cytoscout software (CBL) at a frame rate of 5 fps. The mean intensities I_M delivered by the fusing vesicle in a 1 μm × 1 μm area centered at the fusion site were determined by a custom-written Matlab program.

Adenovirus Infection and Transmission Electron Microscopic analysis. Polystyrene filter-grown polarized MDCK monolayers were infected with adenovirus from the basolateral surfaces for 3 h, as previously described (11). To perform transmission electron microscopic (TEM) analysis, we optimized the conditions so that >90% cells exhibited increased dyn2 signal 1 d after infection. Cells were rinsed with warm DMEM and PBS/Ca/Mg, and then fixed in 4% (wt/vol) paraformaldehyde for 10 min. At this time point, cells were processed for conventional TEM analysis (12) or immuno-EM (13) as described with minor modifications. For immunolocalization of Rab11a, fixed cells were incubated with Rab11a antibody in 0.5% BSA/PBS followed by 5 nm gold-conjugated secondary antibody and followed by postfixation in 2% (wt/vol) glutaraldehyde for 10 min, washed, and submerged in 2% (wt/vol) osmium tetroxide for 1 h. After thorough washes in 0.1 M phosphate buffer, filters were dehydrated in graded ethanol series, followed by propylene oxide, and embedded in Epon resin in a flat mold. Blocks were baked at 60 degrees for 3 d before ultrathin sectioning, followed by counterstaining with uranyl acetate and lead citrate. Samples were viewed with a CM10 electron microscope (Philips).

1. Ceresa BP, Kao AW, Santeler SR, Pessin JE (1998) Inhibition of clathrin-mediated endocytosis selectively attenuates specific insulin receptor signal transduction pathways. *Mol Cell Biol* 18(7):3862–3870.
2. Yeh TY, Peretti D, Chuang JZ, Rodriguez-Boulan E, Sung CH (2006) Regulatory dissociation of Tctex-1 light chain from dynein complex is essential for the apical delivery of rhodopsin. *Traffic* 7(11):1495–1502.
3. Butterworth MB, et al. (2012) Rab11b regulates the trafficking and recycling of the epithelial sodium channel (ENaC). *Am J Physiol Renal Physiol* 302(5):F581–F590.
4. Deborde S, et al. (2008) Clathrin is a key regulator of basolateral polarity. *Nature* 452(7188):719–723.
5. Wiznerowicz M, Trono D (2003) Conditional suppression of cellular genes: Lentivirus vector-mediated drug-inducible RNA interference. *J Virol* 77(16):8957–8961.
6. Gibson DG, et al. (2009) Enzymatic assembly of DNA molecules up to several hundred kilobases. *Nat Methods* 6(5):343–345.
7. Chua J, Rikhy R, Lippincott-Schwartz J (2009) Dynamin 2 orchestrates the global actomyosin cytoskeleton for epithelial maintenance and apical constriction. *Proc Natl Acad Sci USA* 106(49):20770–20775.
8. Dunn KW, Kamocka MM, McDonald JH (2011) A practical guide to evaluating colocalization in biological microscopy. *Am J Physiol Cell Physiol* 300(4): C723–C742.
9. Thuenauer R, et al. (2011) A PDMS-based biochip with integrated sub-micrometre position control for TIRF microscopy of the apical cell membrane. *Lab Chip* 11(18): 3064–3071.
10. Paar C, et al. (2008) High throughput FRET screening of the plasma membrane based on TIRFM. *Cytometry A* 73(5):442–450.
11. Tai AW, Chuang JZ, Sung CH (2001) Cytoplasmic dynein regulation by subunit heterogeneity and its role in apical transport. *J Cell Biol* 153(7):1499–1509.
12. Haller C, Schick CS, Zorn M, Kübler W (1997) Cytotoxicity of radiocontrast agents on polarized renal epithelial cell monolayers. *Cardiovasc Res* 33(3):655–665.
13. Hagiwara H, Aoki T, Suzuki T, Takata K (2010) Pre-embedding immunoelectron microscopy of chemically fixed mammalian tissue culture cells. *Methods Mol Biol* 657: 145–154.
14. Marks B, et al. (2001) GTPase activity of dynamin and resulting conformation change are essential for endocytosis. *Nature* 410(6825):231–235.

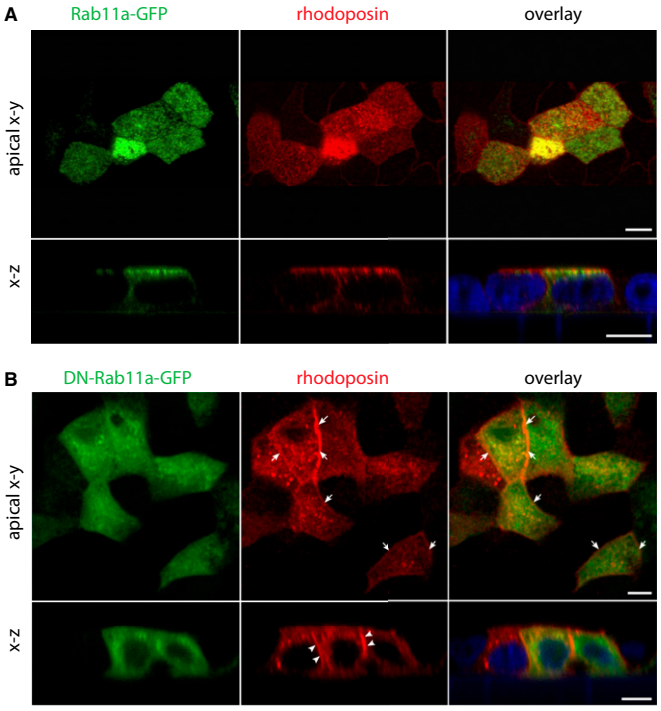

Fig. S1. Dominant negative Rab11a interferes with apical targeting of untagged rhodopsin. MDCK cells were transfected with untagged rhodopsin (red) and Rab11a-GFP (*A*) or DN-Rab11a-GFP (*B*) using electroporation. Next, 1×10^5 cells were seeded on 24-well Transwell filters and allowed to polarize for 4 d. The cells were fixed, permeabilized, and immunostained with the primary antirhodopsin antibody B6-30 and Alexa568-conjugated secondary antibody. Apical *x–y* and vertical *x–z* sections from confocal image stacks are shown. Arrows (*x–y* planes) and arrowheads (*x–z* planes) point to the lateral signal of mistrafficked rhodopsin in cells cotransfected with DN-Rab11a-GFP. (Scale bars, 10 μm.)

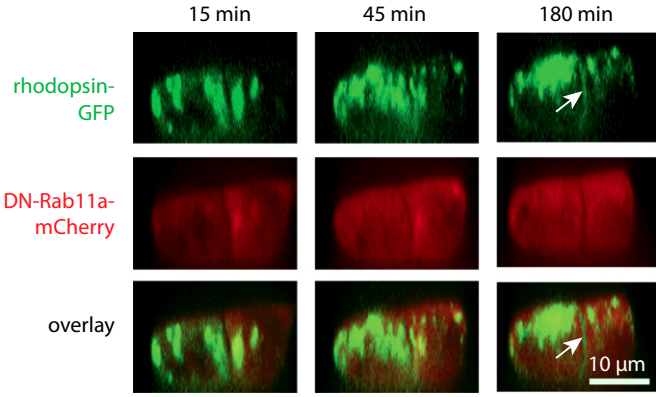

Fig. S2. Rab11a is required for the apical plasma membrane (PM) arrival of rhodopsin-GFP. Immediately after the addition of AP21998 (defined as t = 0 min), polarized MDCK cells transfected with FM4-rhodopsin-GFP and DN-Rab11a-mCherry were transferred to the microscope and imaging was initiated. Representative sections along the apico–basal axis of two cells are shown. Note that rhodopsin-GFP signal appears at the basolateral PM after 180 min of release (arrows).

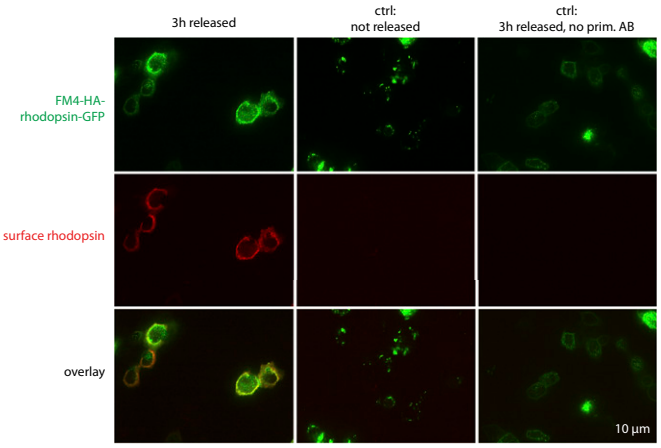

Fig. S3. Validation of detection method for surface targeting of rhodopsin using FM4-HA-rhodopsin-GFP. Three hours after AP21998 release, subconfluent MDCK cells transfected with FM4-HA-rhodopsin-GFP were fixed in 1% paraformaldehyde. These cells were stained under nonpermeablizing conditions with anti-HA antibody followed by Cy5-conjugated secondary antibody to detect surface rhodopsin. Note that no surface rhodopsin is visible in control samples that have not been treated with AP21998 (ctrl: not released) or in samples that were released and did receive only secondary Cy5-conjugated antibody, but no primary anti-HA antibody (ctrl: 3 h released, no prim. AB).

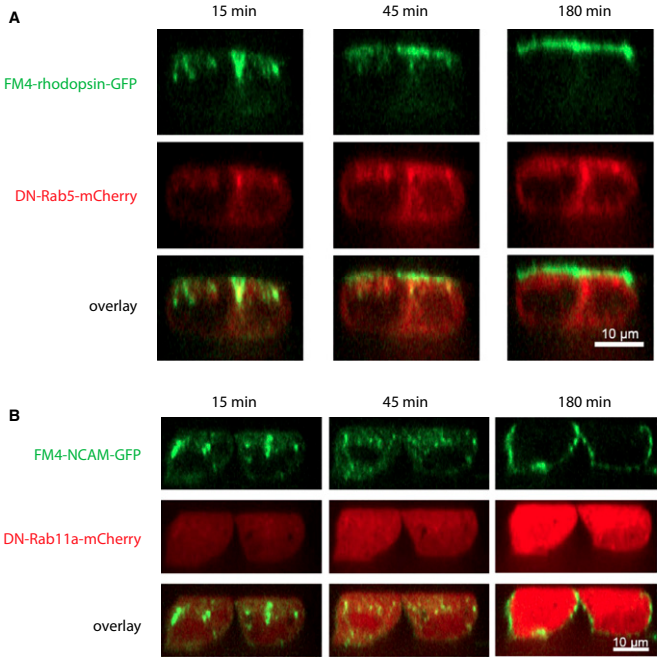

Fig. S4. Control experiments demonstrating the specific involvement of Rab11a in rhodopsin apical PM delivery. Time lapse confocal images of polarized MDCK cells cotransfected with FM4-rhodopsin-GFP and DN-Rab5-mCherry (*A*) or FM4-NCAM-GFP and DN-Rab11a-mCherry (*B*), and treated with AP21998 (start of treatment defined as t = 0 min). Representative sections along the apico–basal axis of two neighboring cells are shown.

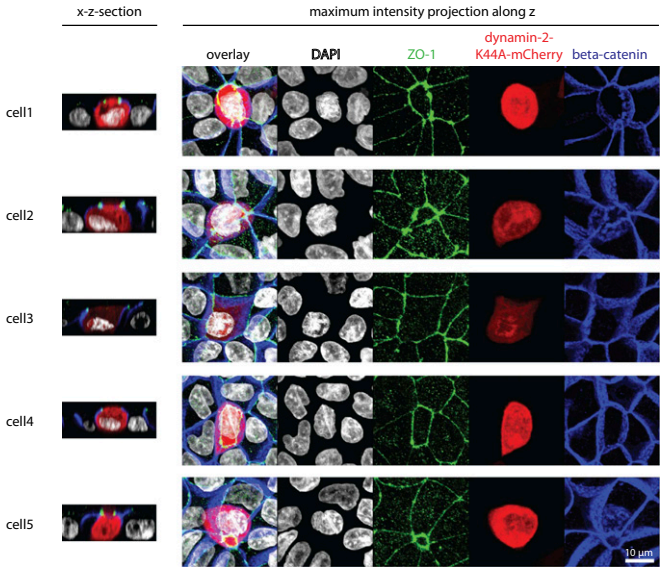

Fig. S5. Overexpression of dominant negative dyn2 does not alter cell polarity. Polarized MDCK cells were transiently transfected with dyn2-K44A-mCherry using exactly the same conditions (e.g., DNA amount, expression time) as used in the experiments for Fig. 4*B*. After fixation, cells were immunostained for the tight junction marker ZO-1 and the basolateral marker beta-catenin. Note that dyn2-K44A-mCherry expression neither compromised tight junction nor changed the basolateral localization of beta-catenin.

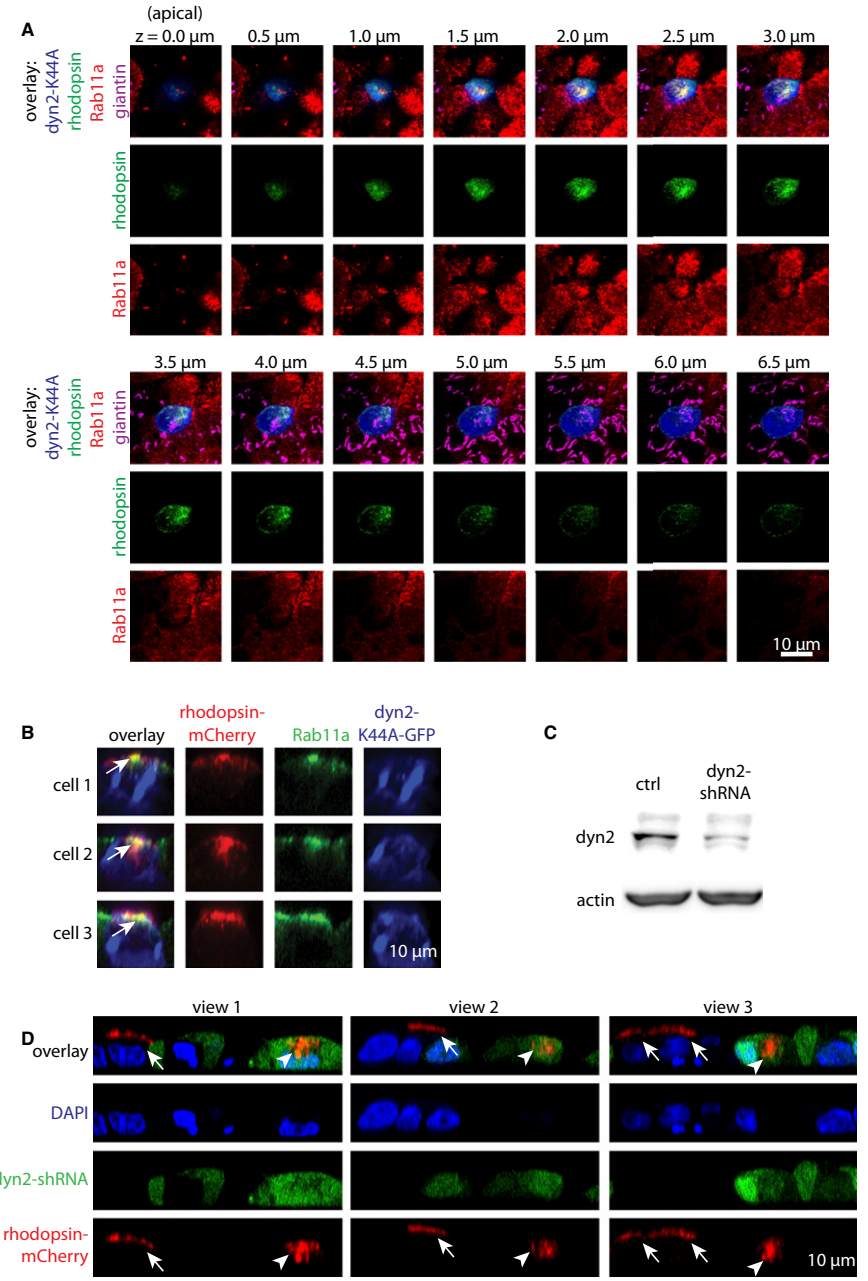

Fig. S6. Dyn2 perturbation induces retention of rhodopsin-mCherry at Rab11a-positive apical recycling endosomes (AREs). (*A*) A stack of *x*–*y* confocal sections (0.5 µm thick) of several untransfected cells surrounding one cell that was transfected with dyn2-K44-mCherry (false color in blue) and rhodopsin-GFP (green) (i.e., "cell 1" from Fig. 4*B*). These fixed cells were also stained for Rab11a (false color in red) and giantin (mangenta). The colocalization of rhodopsin-GFP with Rab11a in the dyn2-K44–expressing cells is apparent in several sectional planes. (*B*) Polarized MDCK cells cotransfected with FM4-rhodopsin-mCherry (red) and dyn2-K44A-GFP (false color in blue) were treated with AP21998 for 3 h, fixed, and immunostained for Rab11a (false color in green). Confocal sections along the apico–basal axis of three representative cells demonstrate an extensive overlap between the signals of rhodopsin and Rab11a. (*C* and *D*) Lentiviral shRNA-mediated knockdown of dyn2. For knockdown, nonpolarized MDCK cells were incubated with lentivirus encoding both GFP and dyn2-shRNA, for 1 d, then seeded on Transwell filters and cultured for 3 d. (*C*) Western blot confirming the shRNA-mediated knockdown of dyn2. (*D*) Dyn2 knockdown interferes with PM targeting of rhodopsin. Transwell filter-grown lentivirus-infected cells were transfected with FM4-rhodopsin-mCherry (red) and released for 3 h with AP21998. After fixation, cells were stained with DAPI (blue) and imaged with a confocal microscope. Three apico–basal cross-sectional views that contain both dyn2-shRNA-lentivirus infected cells (green) and noninfected cells, are shown. Note that in nonlentivirus-infected cells rhodopsin-mCherry (white arrows) reaches the PM, whereas in lentivirus-infected cells (white arrowheads), rhodopsin-mCherry is retained in the cytosol.

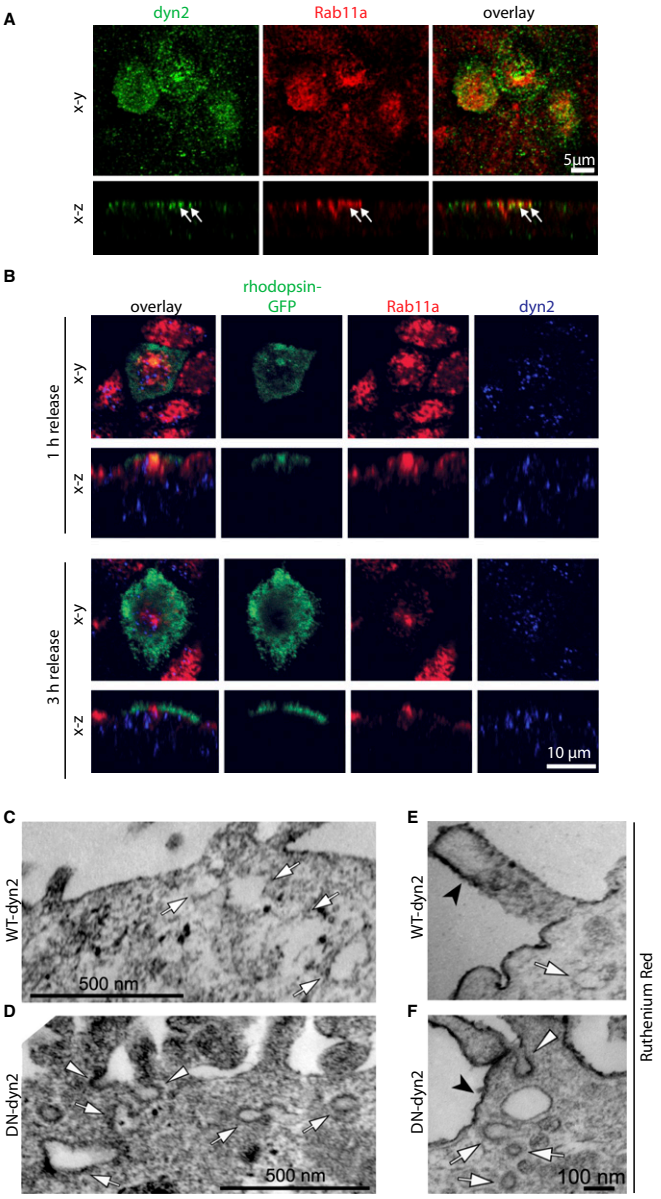

Fig. S7. Dyn2 control experiments. (*A*) Polarized MDCK monolayers were infected with adenovirus encoding dyn2-WT for 1 d (~50% cells were infected in this experiment), fixed, and immunolabeled for dyn2 and Rab11a. White arrows point to the overlapping signals derived from ectopically expressed dyn2 (which exhibited brighter signal than endogenous dyn2) and Rab11a. (*B*) Polarized MDCK monolayers transiently transfected with FM4-rhodopsin-GFP were released by AP21998 for 1 h or 3 h, fixed, and immunolabeled for endogenous Rab11a and dyn2. (*C* and *D*) Conventional TEM was performed on MDCK monolayers similar to Fig. 4 *D* and *E* except the antibody incubation was omitted. Representative electron micrographs of polarized MDCK cells expressing WT-dyn2 (*C*) or DN-dyn2 (*D*). Arrowheads in *D* point to coated pits accumulated on the PM. Characteristic coats were also frequently found on subapical tubular structures (arrows) of DN-dyn2, but not WT-dyn2 expressing cells. (*E* and *F*) Electron micrographs of polarized MDCK cells expressing WT-dyn2 (*E*) or DN-dyn2 (*F*) that were labeled with 0.5 mg/mL ruthenium red during fixation [4% (wt/vol) paraformaldehyde and 2% (wt/vol) osmium tetroxide] (14). In both conditions ruthenium red reaction products cover the outer surfaces of the cells including the microvilli (black arrowheads). White arrowhead in *F* points to a coated pit arrested on a ruthenium red-labeled PM invagination. Coated structures were also frequently found on ruthenium red-devoid subapical compartments (white arrows) of DN-dyn2 (*F*), but not WT-dyn2 (*E*) expressing cells.

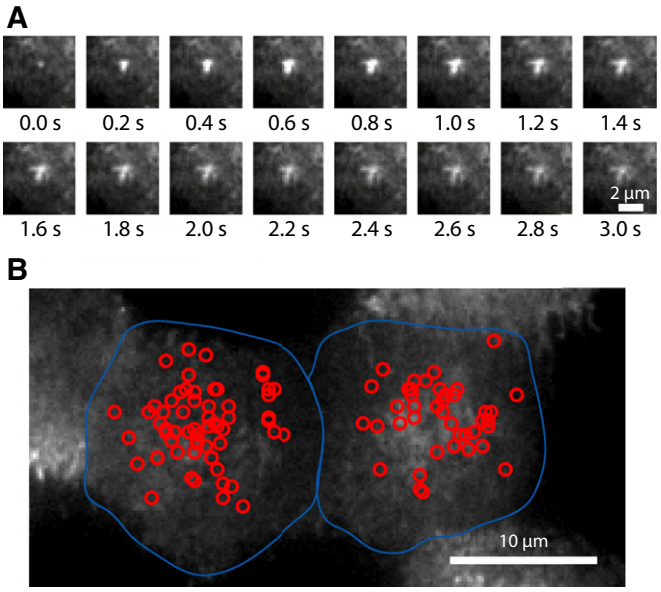

Fig. S8. Characterization of apical fusion events of rhodopsin-GFP–bearing vesicles. (*A*) Time-lapse images of a rhodopsin-GFP–bearing vesicle undergoing fusion with the apical PM and showing noncircular spreading of rhodopsin-GFP after fusion onset. The diffusive spreading of the rhodopsin-GFP molecules after fusion appears to occur along three microvilli, suggesting that this vesicle fused at the base of these microvilli. (*B*) Distribution of fusion events of rhodopsin-GFP–bearing vesicles (red circles) at the apical PM of two MDCK cells (outlined by blue lines) as recorded during a 12-min time period.

A (Rab11a)

B (Rab11b)

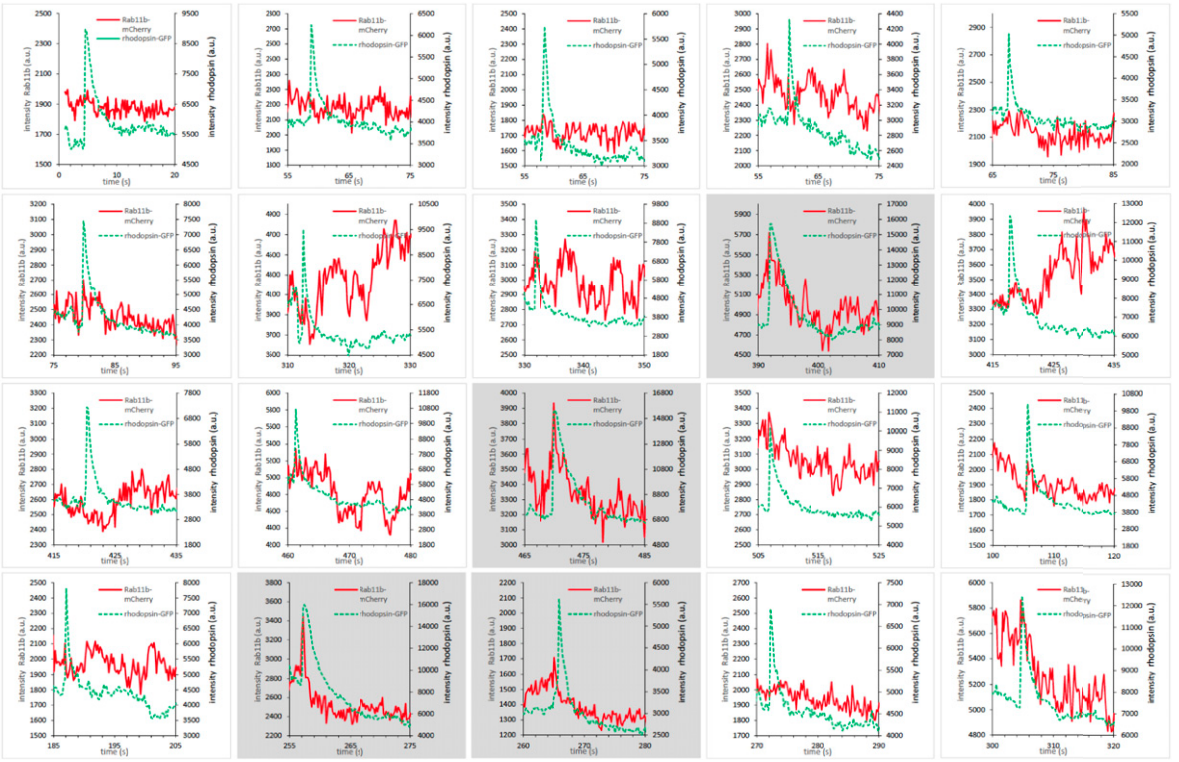

Fig. S9. Analysis of Rab11a and Rab11b occurrence on fusing rhodopsin-GFP–bearing vesicles. Subconfluent MDCK cells were transiently transfected with FM4-rhodopsin-GFP together with either Rab11a-mCherry (*A*) or Rab11b-mCherry (*B*). Vesicle fusion events were imaged at the adherent membrane with dual-color TIRFM after AP21998 release. The time course graphs of the mean intensity measured at an 1 μm × 1 μm region centered at the fusion site for the rhodopsin-GFP signal and the signal of Rab11a-mCherry (*A*) or Rab11b-mCherry (*B*) from 20 randomly chosen fusion events are shown. Events that show a correlation between the GFP and mCherry signal are underlayed with gray background.

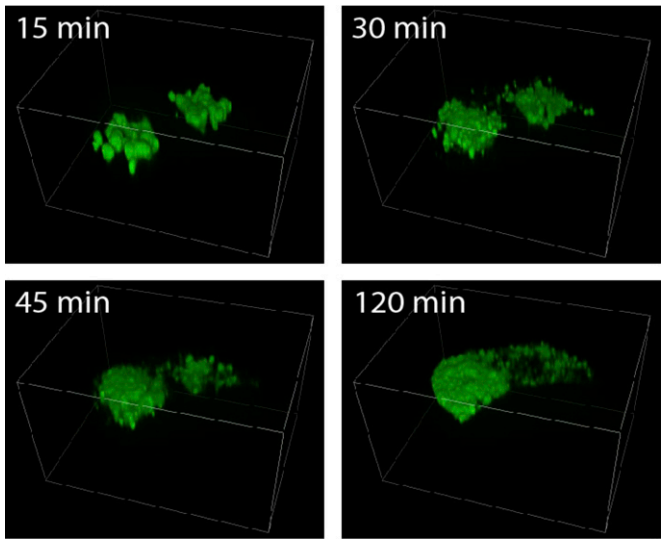

Movie S1. A 3D time-lapse representation of apical trafficking of FM4-rhodopsin-GFP in polarized MDCK cells. Filter grown MDCK cells were transiently transfected with FM4-rhodopsin-GFP using Lipofectamine 2000. Next, filters were cut out and placed on a glass coverslip in recording medium. The cells were transferred to a spinning disk confocal microscope and imaging was initiated 15 min after addition of AP21998.

Movie S1